TITLE PAGE

Citation Format:

L. Di Sieno, T. Talala, E. Avanzi, I. Nissinen, J. Nissinen, A. Dalla Mora, "Towards time-domain diffuse optics with extreme photon rate," Proc. SPIE 12628, Diffuse Optical Spectroscopy and Imaging IX, 1262815 (9 August 2023).

Copyright notice:

DOI abstract link:

https://doi.org/10.1117/12.2669264

Towards time-domain diffuse optics with extreme photon rate

L. Di Sieno*[a], T. Talala[b], E. Avanzi[a], I. Nissinen[b], J. Nissinen[b], A. Dalla Mora[a]
[a]Politecnico di Milano - Dipartimento di Fisica, Milano, Italy;
[b]University of Oulu - Circuits and Systems Research Unit, Oulu, Finland.

ABSTRACT

We present the application to time-domain diffuse optics of a device composed of 8x256 CMOS SPAD array with 256 7-bit time-to-digital converters. Thanks to its structure and despite the limitation on the maximum repetition rate of the laser (2 MHz), it has been demonstrated to be suitable for fast acquisitions (10 ms) provided that a high photon count-rate is used and pile-up distortion is corrected. We demonstrate that high penetration depth (>30 mm) and good linearity in absorption coefficient retrieval can be achieved. Finally, we were able to clearly record the heart beat in a resting state forehead measurement.

Keywords: diffuse optical spectroscopy, light scattering, high count-rate, fast dynamics

1. INTRODUCTION

Among different implementations of Diffuse Optics (DO) for tissue imaging and spectroscopy, the Time-Domain (TD) is recognized as the most informative one, mainly due to intrinsic capability to disentangle absorption from scattering information and to probe different depths in the tissue by analyzing photons at different arrival times [1]. On the other hand, TD-DO is historically impaired by high cost and size of the required components [2], as well as a low Signal-to-Noise Ratio (SNR) due to the need for Time-Correlated Single-Photon Counting (TCSPC) acquisitions, preventing the possibility to perform fast measurements, thus typically limiting the sampling rate to ~10 Hz [3].

Recently, devices miniaturization by several orders of magnitude has been obtained by different researchers (see e.g., [4],[5]), as well as an increased measurement rate, thus permitting for instance to distinguish the heart beat pattern in functional Near-Infrared Spectroscopy (fNIRS) applications (see e.g., [4],[6]), as already widely achieved by continuous wave DO. In Ref. [6], using state-of-the-art bulky technologies, it has been achieved an acquisition rate of 20 Hz by using a detection chain with responsivity [7] of 2.8 10^{-8} m^2sr at about 690 nm and a laser pulsing rate of 80 MHz. Instead, Ref. [4], by using miniaturized technologies, demonstrated a much larger sampling rate of 200 Hz, using a detection chain with a responsivity of 7.2 10^{-9} m^2sr at the same wavelength and a laser pulsing rate of 20 MHz.

As a matter of fact, the capability to follow fast tissue dynamics requires both a high measurement rate and a high SNR resulting from a large detection chain responsivity. In this work, we present the characterization and preliminary in-vivo use of a proof-of-concept miniaturized detection chain capable of working at high sampling rates (~100 Hz) and featuring superior responsivity (2.27 10^{-7} m^2sr at about 670 nm). Thanks to the latter, we also exploit its operation beyond the pile-up limit of TCSPC to further boost the SNR. With respect to previous works, here a single wavelength is used, preventing for now the possibility to disentangle oxy- and deoxy-hemoglobin. However, it has been possible to achieve a Photon Counting Rate (PCR) >400M of counts per second (cps) for a single detection point at a source-detector distance of about 20 mm on human tissues, while, to the best of our knowledge, other high PCR systems at the same distance practically achieved in-vivo a median PCR across different detectors of <20 Mcps due to the lower responsivity [4] or to hardware limitations [6]. This result has been obtained despite the use of a low laser pulse rate (just 2 MHz), which is forced by limitations of the present version of the integrated circuit (initially devised for other applications), thus easily anticipating a further increase in the PCR up to several Gcps thanks to a tailored microelectronic design.

* laura.disieno@polimi.it; phone +39 02 2399 6597; fax +39 02 2399 6126; https://www.fisi.polimi.it/en/user/1097

Diffuse Optical Spectroscopy and Imaging IX, edited by Davide Contini, Yoko Hoshi, Thomas D. O'Sullivan, Proc. of SPIE Vol. 12628, 1262815
 · 0277-786X · doi: 10.1117/12.2669264

2. MATERIALS AND METHODS

Our setup was composed of a laser source at 670 nm (PDL 828 Sepia II with LDH-P-C-670M, Picoquant GmbH, Germany). The emitted light was directly coupled to an optical fiber, acting as the input of a fiber-to-fiber u-bench where a variable optical attenuator was placed to set the proper count-rate. Light was then shone on the sample under analysis. As detection chain, we used the chip described in Ref. [8], composed of 8x256 CMOS SPADs and 256 7-bit Time-to-Digital Converters (TDCs), each one reading a line of 8 SPADs and with a time bin of about 60 ps . The repetition rate of the laser was limited to 2 MHz since the chip cannot operate at higher frequency. To objectively characterize the device, we adopted some tests of well-established protocols for performance assessment of diffuse optics systems [7] such as Instrument Response Function shape (IRF) and responsivity (i.e., light harvesting capability) from Basic Instrumental Performance (BIP) protocol; contrast (i.e., the relative change in the number of photon due to the presence of optical inhomogeneity) and Contrast-to-Noise-Ratio (CNR, i.e., the robustness of the contrast with respect to the intrinsic fluctuation of the measurement) from nEUROPt protocol; and the linearity in the retrieval of absorption coefficient in homogeneous samples from MEDPHOT protocol. Except for the responsivity, all measurements were performed at two different PCRs: one within and one well beyond the single photon statistics (60 k -i.e., 3% of the laser pulsing rate- and 1.7 M -i.e., 85% of the laser pulsing rate- counts per second on the single TDC, respectively). In the latter case, a simple yet effective algorithm for correction of pile-up effect has been applied as a first step [9]. In all measurements, the distribution of time-of-flight recorded by the 256 TDCs has been summed up and then the background value has been subtracted.

For what concerns the implementation of the above-mentioned test (excluded the responsivity), we decide to use 100 repetitions of 10 ms for both PCRs. For the contrast and CNR, we used a liquid phantom featuring homogeneous optical properties of 0.1 cm^{-1} and 10 cm^{-1} as absorption (μ_a) and reduced scattering (μ_s') respectively. As absorption inhomogeneity we used a totally absorbing inclusion which is equivalent to a $\Delta\mu_a$ of 0.17 cm^{-1} over 1 cm^3.

As a last step, we used our probe to measure the forehead in resting condition to check if the heartbeat can be seen. To avoid signal coming from the superficial layer, the probe was pressed to minimize the heartbeat effect in the scalp [10]. Measurements at 10 ms were acquired for about 1 min, then after pile-up correction and background subtraction, suitable filtering was applied to enhance the visibility of fast oscillations with respect to the Poisson noise. Finally, a discrete Fast Fourier Transform (FFT) was applied to recover the frequencies dominating the signal.

3. RESULTS, DISCUSSION AND CONCLUSIONS

The responsivity was measured to be 2.27 10^{-7} m^2sr, showing an improvement of almost decade with respect to high sample rate instrument featuring the highest responsivity [6]. The improved responsivity will increase the collected signal thus possibly improving the achievable performances in terms of depth sensitivity. The contrast and CNR achieved with the proposed detector in a late time gate of 500 ps width (about 4.8 ns from the pulse injection) are reported in Figure 1. As expected, the contrast does not change significantly with the PCR while the CNR improves for above-statistics acquisitions [9]. Thanks to the improvement in the CNR, the penetration depth (usually considered as the last point were both contrast> 1% and CNR >1) passes from 27.5 to 32.5 mm when using the high PCR thus confirming this approach.

Moreover, we verified that the use of well-above statistics PCR, does not affect the capability of the system to properly retrieve the optical properties of an homogeneous medium. Indeed, Figure 2(a) reports the linearity in the retrieval of absorption coefficient for the series of phantoms featuring a μ_s'= 5 cm^{-1}. It is clear that the use of standard or a high PCR does not affect the capability to recover linear variation in μ_a, provided that in the latter case a suitable pile-up correction is applied [9].

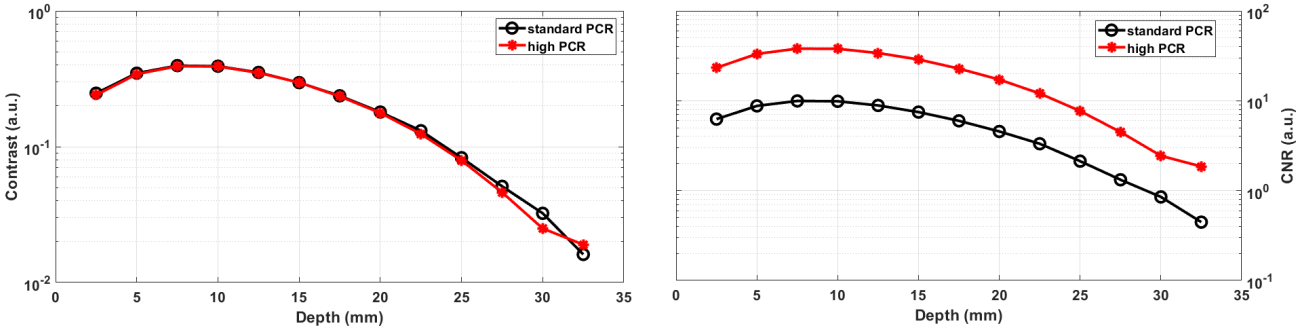

Figure 1. *Contrast (left) and CNR (right) obtained using the standard and the high PCR (black and red curves, respectively).*

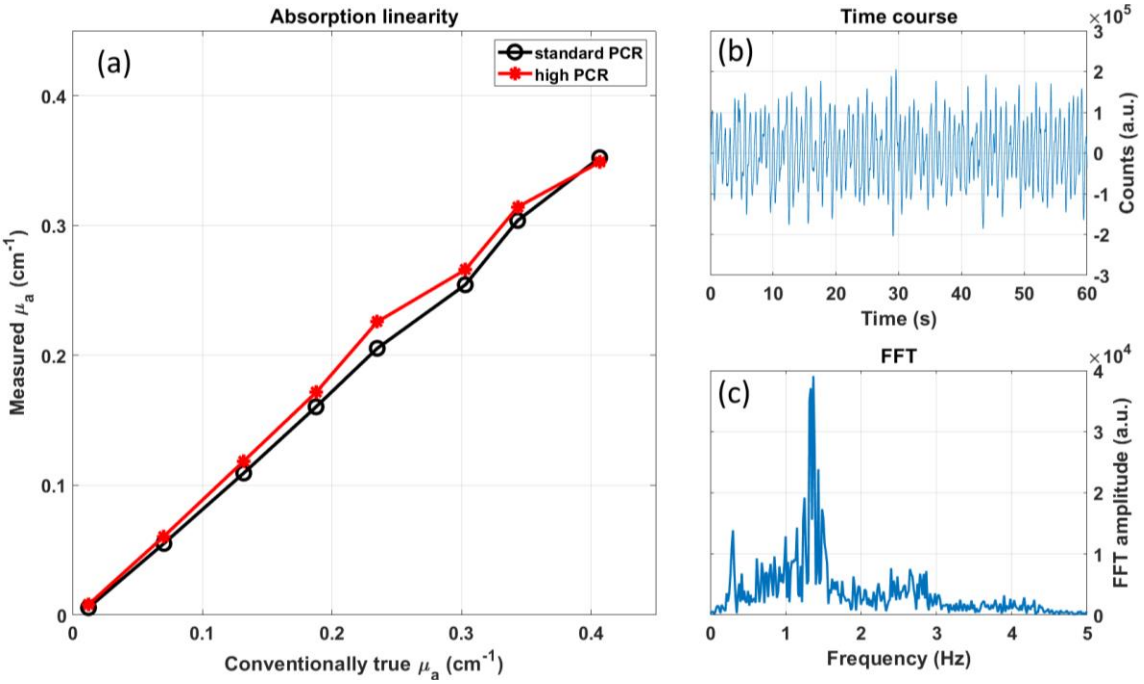

***Figure 2**. (a) Linearity of absorption coefficients retrieval from MEDPHOT protocol obtained using the standard and the high PCR (black and red curves, respectively); (b) time course of the filtered signal acquired on the forehead and (c) its FFT analysis.*

Figure 2(b) and (c) reports, respectively, the filtered signal obtained from forehead measurements and the spectral components obtained from FFT. It is clearly visible that a periodical signal can be recorded and, being its main contribution at 1.4 Hz (i.e., around 84 beats per minute), it is compatible with the heartbeat.
In future, overcoming the limitation in the maximum repetition rate of the laser (reaching tens of MHz), will allow to further reduce the integration time (down to 1 ms or less) thus opening the way to the recording of fast dynamics or to the speed-up of spectral measurements (e.g., for optical mammography).

ACKNOWLEDGEMENTS

This work was supported by the Laserlab-Europe EU-H2020 871124 project and by the Academy of Finland, under Contracts 323719 and 330121. The authors would like to acknowledge Fondazione Bruno Kessler for designing the SPAD devices used in this work.

REFERENCES

[1] Durduran, T. et al, “Diffuse optics for tissue monitoring and tomography”, Rep Prog Phys 73(7), 076701 (2010)
[2] Pifferi, A. et al, “New frontiers in time-domain diffuse optics, a review”, J Biomed Opt, 21(9), 091310 (2016)
[3] Applegate, M.B. et al, “Recent advances in high speed diffuse optical imaging in biomedicine”, APL Phot 5, 040802 (2016)
[4] Ban, H.Y. et al, “Kernel Flow: a high channel count scalable time-domain functional near-infrared spectroscopy system”, J Biomed Opt, 27(7), 074710 (2022)
[5] Di Sieno, L. et al, “First in-vivo diffuse optics application of a time-domain multiwavelength wearable optode”, Biophotonics Congress: Biomedical Optics 2022 (Translational, Microscopy, OCT, OTS, BRAIN), paper OTu4D.3 (2022).
[6] Re, R. et al, “Reliable fast (20 Hz) acquisition rate by a TD fNIRS device: brain resting-state oscillation studies”, Sensors 23(1), 196 (2022)
[7] Dalla Mora, A. et al, “The SiPM revolution in time-domain diffuse optics”, Nucl Instrum Meth A 978, 164411 (2020)
[8] Talala, T. et al, “CMOS SPAD Line Sensor With Fine-Tunable Parallel Connected Time-to-Digital Converters for Raman Spectroscopy”, IEEE J Solid-St Circ, Early Access 20 Oct. (2022)
[9] Avanzi, E. et al, “Effects and correctability of pile-up distortion using established figures of merit in time-domain diffuse optics at extreme photon rates”, Sci Rep-UK 12(1), 1–12 (2022)
[10] Pagliazzi, M. et al., “Time resolved speckle contrast optical spectroscopy at quasi-null source-detector separation for non-invasive measurement of microvascular blood flow”. Biomed. Opt. Express, 12 (3), 1499–1511 (2021).